Hindawi
Advances in Materials Science and Engineering
Volume 2019, Article ID 1354065, 9 pages
https://doi.org/10.1155/2019/1354065

Research Article

Probability of Exceeding Damage States in Plates Using BEM

Ernesto Pineda-León,[1] **José Manuel Rosales-Juárez**,[2] **Dante Tolentino**,[3] **and Orlando Susarrey-Huerta**[2]

[1]*Sección de Estudios de Posgrado e Investigación, ESIA Zacatenco, Instituto Politécnico Nacional, Mexico City, Mexico*
[2]*Sección de Estudios de Posgrado e Investigación, ESIME Zacatenco, Instituto Politécnico Nacional, Mexico City, Mexico*
[3]*Departamento de Materiales, Universidad Autónoma Metropolitana, Mexico City, Mexico*

Correspondence should be addressed to Dante Tolentino; dantetl@azc.uam.mx

Received 21 February 2019; Revised 28 August 2019; Accepted 1 November 2019; Published 21 November 2019

Academic Editor: Kenji Kaneko

Copyright © 2019 Ernesto Pineda-León et al. This is an open access article distributed under the Creative Commons Attribution License, which permits unrestricted use, distribution, and reproduction in any medium, provided the original work is properly cited.

An approach to obtain fragility curves taking into account the formulation for shear deformable plate theory with combined geometric and material nonlinearities and the boundary element method is proposed. It is assumed that the material undergoes large deflection with small strains. The von Mises yield criterion is used to evaluate the plastic zone and is supposed to have elastic-perfectly plastic material behaviour. An initial stress formulation is used to formulate the boundary integral equations. The domain integrals are evaluated using a cell discretization technique. A total incremental method is applied to solve the nonlinear boundary integral equations. The approach is illustrated in a plate subjected to incremental load. The uncertainties in both geometric and mechanical properties are considered in order to obtain the structural response. Results show that there are high probabilities of exceeding the damage state, d, equal to 0.05 while for the rest of the values of d, these probabilities are low.

1. Introduction

Plates are structural elements of great importance because they are used to characterize multiple mechanical conditions. Due to this, their analysis and prediction under different conditions and behaviours are of vital importance in their design. The probability that certain parameters exceed limits that could lead to failure takes an important role in determining such safety indicators in its design, for which probabilistic analyses help to find appropriate values for those parameters.

Kirchhoff [1] developed a theory that is currently widely used and is commonly known as the classical theory of plates. Reissner [2] on the other hand, enriched the classical theory with shear deformation contributions on the plate. In general, the classical theory provides good approximations when analysing some cases; however, for situations where the modelling of the stress concentration is required, this theory is not appropriate because it omits the shear deformations. In the theory proposed by Reissner, the problem is modelled in terms of three degrees of freedom that includes the generalized displacements and tractions.

In the last three decades, the Boundary Element Method (BEM) has emerged as a powerful numerical tool for plate analyses [3]. With this technique, some analyses have been developed in order to solve linear elastic behaviours on plates [4, 5]. The boundary integral equation for the model of the Reissner plate was presented in the work of Weeën [6]. Later, Karam and Telles [7] extended the formulation for infinite regions and reported that this theory is suitable for thin and thick plates. Recent works regarding plates can be found in [8].

A thin plate can suffer large deflections with normal service loads. In such cases, the behaviour cannot be adequately described using the theory of small elastic deformations. When that deflection in the plate is equal or bigger than its thickness, effects of nonlinearity occurs due to the coupling of forces and deflections in equilibrium conditions. Some works that deal with the geometrical linearity in plates using the classical theory can be found in [9–14]. Dirgantara and Aliabadi [15] reported the application of BEM for large deformations in shells. Purbolaksono and Aliabadi [14] used this method in a plate under shear deformation where they showed two methods to calculate the derivatives of the nonlinear terms in the domain integral. To solve the nonlinear problem, they concluded that the most efficient approach is the method of total increase proposed by Wen et al. [13].

Karam and Telles [16] introduced a BEM formulation for the elastoplastic analysis of Reissner plates where the classical theory of plasticity was used. The combination of geometric and material nonlinear analysis in 2D problems using BEM was first presented by Chandra and Mukherjee [17], and in this work he analysed large deformations for an isotropic material. Supriyono and Aliabadi [18] made a new formulation of boundary integral equations for combined geometric and material nonlinearities of shear deformable plate-bending analysis. The cell discretization approach is used for evaluating the domain integrals, and the total increment method is used for the nonlinear boundary integral equations, the same as was presented by [13].

On the other hand, there are different factors that affect the response of a certain structure such as manufacturing errors that could change both mechanical and geometrical properties. So, the loads to which the structure could be exposed are variable in magnitude, occurrence, duration, etc. This implies to consider all possible parameters as stochastic variables that affect the response of the structural element subjected to a certain load. According to this, several authors such as Rahman and Chen [19] and Huang and Aliabadi [20] have used the BEM method for probabilistic analysis in order to solve crack problems, elastic-linear problems [21–23], elastostatic problems [24–27], and optimization problems [28]. Fragility curves have been estimated in some kind of structural systems such as bridges, buildings, and transmission towers under different loads, i.e., seismic [29–33], wind [34, 35], and tsunami [36]. Unfortunately, the mentioned approaches have not used BEM to obtain fragility curves that represent the probability of exceeding a certain damage state considering the uncertainties related to both mechanical and geometrical properties of the structural element.

It is important to take into account since the load is increasing, and the probability of exceeding a certain established damage threshold increases. When the probability of exceeding a certain threshold is known before all possible loads, decisions can be made on the structural element through redesign or, if appropriate, verifying that the proposed element will develop a proper behaviour.

This research presents an approach to obtain fragility curves using BEM that takes into account the combination of large deformations and plasticity using the formulations shown in the work of Supriyono and Aliabadi [18]. The uncertainties related with mechanical (modulus of elasticity, yield stress, and ultimate stress) and geometric (thickness, base, height) properties were considered. So, different damage states were selected to estimate the probability of being exceeded. A simple supported plate at its ends with uniformly distributed load increased in every step was used for the analysis.

2. Formulation

2.1. Governing Equations. The relationships between stress resultants and strains by using the Reissner's variational theorem of elasticity are shown in [29]. The development to get this formulation can be reviewed in [18]. Then, the relationship can be written as

$$\begin{aligned}\mu_{xy} &= D\frac{1-\nu}{2}\left(2\chi_{xy} + \frac{2\nu}{1-\nu}\chi_{\gamma\gamma}\delta_{xy}\right) - \mu^{p}_{xy},\\ \eta_{xy} &= B\frac{1-\nu}{2}\left(\varepsilon_{xy} + \varepsilon_{yx} + \frac{2\nu}{1-\nu}\varepsilon_{\gamma\gamma}\delta_{xy}\right) - \eta^{p}_{xy},\\ \varphi_x &= C\gamma_{x3},\end{aligned} \tag{1}$$

where $D = Eh^3/(1-\nu^2)$, $B = Eh/(1-\nu^2)$, and $C = Ekh/(2(1+\nu))$, $k = 5/6$.

The equilibrium equations are

$$\begin{aligned}\mu_{xy,x} - \varphi_x &= 0,\\ \varphi_{x,x} + \left(\eta_{xy}w_{3,y}\right)_{,x} + q_3 &= 0,\\ \eta_{xy,y} &= 0,\end{aligned} \tag{2}$$

where μ_{xy}, φ_x, and η_{xy} are the moment stress resultants, the shear stress resultants, and membrane stress resultants, respectively. q_3 is uniform load per unit area in the x_3 direction.

2.2. Displacement Integral Equations. The following are the displacement boundary integral equations for the membrane and the plate, see [18]. These can be written for the plate as

$$\begin{aligned}c_{ij}w_i(\mathbf{X}') \pm \int_\Gamma P^*_{ij}(\mathbf{X}',\mathbf{x})w_j(\mathbf{x})d\Gamma = &\int_\Gamma W^*_{ij}(\mathbf{X}',\mathbf{x})p_j(\mathbf{x})d\Gamma\\ &- \int_\Omega W^*_{i3,x}(\mathbf{X}',\mathbf{X})\left(\eta_{xy}w_{3,y}\right)\\ &\times(\mathbf{X})d\Omega\\ &+ \int_\Omega W^*_{i3}(\mathbf{X}',\mathbf{X})q_3(\mathbf{X})d\Omega\\ &+ \int_\Omega \chi^*_{ixy}(\mathbf{X}',\mathbf{X})\mu^{p}{}_{xy}(\mathbf{X})d\Omega.\end{aligned} \tag{3}$$

Also, for the membrane, these can be written as

$$\begin{aligned}c_{\theta x}u_\theta(\mathbf{X}') + \int_\Gamma T^*_{\theta x}(\mathbf{X}',\mathbf{x})u_x(\mathbf{x})d\Gamma = &\int_\Gamma U^*_{\theta x}(\mathbf{X}',\mathbf{x})t_x(\mathbf{x})d\Gamma\\ &- \int_\Omega U^*_{\theta x,y}(\mathbf{X}',\mathbf{X})\eta^{nl}_{xy}(\mathbf{X})d\Omega\\ &+ \int_\Omega \varepsilon^*_{\theta xy}(\mathbf{X}',\mathbf{X})\eta^{p}_{xy}(\mathbf{X})d\Omega,\end{aligned} \tag{4}$$

where $\int$ denotes a Cauchy principal value integral, and c_{ij} are the jump terms. Equations (3) and (4) constitute the boundary displacement integral equations for plate bending problem.

2.3. Stress Integral Equations. As is shown in [18], the stress integral equations for moment stress resultants can be stated as

$$\mu_{xy}(\mathbf{X}') = \int_\Gamma W^*_{xyk}(\mathbf{X}',\mathbf{x})p_k(\mathbf{x})d\Gamma - \int_\Gamma P^*_{xyk}(\mathbf{X}',\mathbf{x})w_k(\mathbf{x})d\Gamma + \int_\Omega W^*_{xy3}(\mathbf{X}',\mathbf{X})q_3(\mathbf{X})d\Omega - \int_\Omega W^*_{xy3,\gamma}(\mathbf{X}',\mathbf{X})\times(\eta_{\gamma y}w_{3,y})(\mathbf{X})d\Omega + \int_\Omega \chi^*_{xy\gamma\theta}(\mathbf{X}',\mathbf{X})\mu^p_{\theta\gamma}(\mathbf{X})d\Omega - \frac{[2(1+\nu)\mu^p_{xy} + (1-3\nu)\mu^p_{\theta\theta}\delta_{xy}]}{8}. \quad (5)$$

Also, the shear stress resultants can be written as

$$\varphi_x(\mathbf{X}')\int_\Gamma W^*_{3yk}(\mathbf{X}',\mathbf{x})p_k(\mathbf{x})d\Gamma - \int_\Gamma P^*_{3yk}(\mathbf{X}',\mathbf{x})w_k(\mathbf{x})d\Gamma + \int_\Omega W^*_{3y3}(\mathbf{X}',\mathbf{X})q_3(\mathrm{X})d\Omega - \int_\Omega W^*_{3y3,\gamma}(\mathbf{X}',\mathbf{X}) \times(\eta_{\gamma y}w_{3,y})(\mathbf{X})d\Omega + \int_\Omega \chi^*_{3y\gamma\theta}(\mathbf{X}',\mathbf{X})\mu^p_{\theta\gamma}(\mathbf{X})d\Omega. \quad (6)$$

Finally, membrane stress resultants can be expressed as

$$\eta_{xy}(\mathbf{X}') = \int_\Gamma U^*_{xy\gamma}(\mathbf{X}',\mathbf{x})t_\gamma(\mathbf{x})d\Gamma - \int_\Gamma T^*_{xy\gamma}(\mathbf{X}',\mathbf{x})u_\gamma(\mathbf{x})d\Gamma - \int_\Omega U^*_{xy\gamma,\theta}(\mathbf{X}',\mathbf{X})\eta^{nl}_{\gamma\theta}(\mathbf{X})d\Omega - \int_\Omega \varepsilon^*_{xy\gamma\theta}(\mathbf{X}',\mathbf{X})\eta^p_{\gamma\theta}(\mathbf{X})d\Omega - \frac{[2(1+\nu)\eta^p_{xy} + (1-3\nu)\eta^p_{\theta\theta}\delta_{xy}]}{8}, \quad (7)$$

where the kernels W^*_{iyk} and P^*_{iyk} are linear combination of the first derivatives of W^*_{ij} and P^*_{ij}, respectively. The kernels $U^*_{xy\gamma}$ and $T^*_{xy\gamma}$ are the linear combination of the first derivatives of U^*_{xy} and T^*_{xy}, respectively. The kernels $\chi^*_{iy\gamma\theta}$ and $\varepsilon^*_{xy\gamma\theta}$ are the linear combination of the first derivatives of χ^*_{ixy} and $\varepsilon^*_{xy\gamma}$, respectively. The free terms appear in equations (5) and (7) arising from using Leibnitz formula. The expressions of the kernels are listed in [37].

2.4. Discretization and System of Equations. The displacement boundary integral equations for membrane and plates mentioned above are discretized, which makes possible to analyze the problem applying the boundary element method. Due to plasticity, it is necessary to discretize the domain Ω into cells and the boundary Γ into boundary elements. For the discretization of the domain nine nodes, quadrilateral quadratic cells were used and the boundary was divided by quadratic isoparametric elements. The corner problems are solved using semidiscontinuous boundary elements, and for the coincident side problems between the boundary and domain, semidiscontinuous cells were applied. In order to avoid the calculation of the deflection derivative on the boundary nodes, the internal values in the nodes of the cells were utilized. To compute the nonlinear terms due to large deflection, it was necessary to use the derivative of the deflection.

Dividing the boundary in quadratic elements and the domain in cells and using the collocation point method, the equations (3) and (4) can be written in a matrix form as follows:

$$\begin{bmatrix}\mathbf{H}^w & 0\\ 0 & \mathbf{H}^u\end{bmatrix}\begin{Bmatrix}w\\ u\end{Bmatrix} = \begin{bmatrix}\mathbf{G}^w & 0\\ 0 & \mathbf{G}^u\end{bmatrix}\begin{Bmatrix}p\\ t\end{Bmatrix} + \begin{Bmatrix}b\\ 0\end{Bmatrix} - \begin{bmatrix}\mathbf{B}^w & 0\\ 0 & \mathbf{B}^u\end{bmatrix} \cdot \begin{Bmatrix}\eta_{\gamma\beta}w_{3,y}\\ \eta^{\gamma y}_{nl}\end{Bmatrix} + \begin{bmatrix}\mathbf{T}^w & 0\\ 0 & \mathbf{T}^u\end{bmatrix}\begin{Bmatrix}\mu^p\\ \eta^p\end{Bmatrix}, \quad (8)$$

where the variables [**H**] and [**G**] are the matrices of influence of boundary elements and [**B**] and [**T**] are the influences for the case of large deflection and plasticity. The plate and the in-plane mode are considered by using w and u. The displacement and traction rate vectors are represented by $\{w\}$, $\{u\}$, $\{p\}$, and $\{t\}$. The variable that represents the load rate vector is $\{b\}$. The stress resultant terms for bending and the membrane are denoted by $\{\mu^p\}$ and $\{\eta^p\}$, respectively. Applying boundary conditions, we obtain the following equation:

$$[A]\{\chi\} = \{\mathbf{f}\} - \begin{bmatrix}\mathbf{B}^w & 0\\ 0 & \mathbf{B}^u\end{bmatrix}\begin{Bmatrix}\eta_{\gamma y}w_{3,y}\\ \dot{\eta}^{nl}_{\gamma y}\end{Bmatrix} + \begin{bmatrix}\mathbf{T}^w & 0\\ 0 & \mathbf{T}^u\end{bmatrix}\begin{Bmatrix}\mu^p\\ \eta^p\end{Bmatrix}, \quad (9)$$

where $[A]$ is the system matrix, $\{\chi\}$ is the unknown vector, and $\{\mathbf{f}\}$ is the vector of prescribed boundary values. Analogously, the stress integral equations can be presented in a matrix form as

$$\begin{Bmatrix}\mu\\ \varphi\\ \eta\end{Bmatrix} = \begin{bmatrix}\mathbf{H}^{w\alpha} & 0\\ \mathbf{H}^{w3} & 0\\ 0 & \mathbf{H}^u\end{bmatrix}\begin{Bmatrix}w\\ u\end{Bmatrix} + \begin{bmatrix}\mathbf{G}^{w\alpha} & 0\\ \mathbf{G}^{w3} & 0\\ 0 & \mathbf{G}^u\end{bmatrix}\begin{Bmatrix}p\\ t\end{Bmatrix} + \begin{Bmatrix}b^\alpha\\ b^3\\ 0\end{Bmatrix} - \begin{bmatrix}\mathbf{B}^{w\alpha} & 0\\ \mathbf{B}^{w3} & 0\\ 0 & \mathbf{B}^u\end{bmatrix}\begin{Bmatrix}\eta_{\gamma\beta}w_{3,y}\\ \eta^{nl}_{\gamma y}\end{Bmatrix} + \begin{bmatrix}\mathbf{T}^{w\alpha}+\mathbf{E}^{w\alpha} & 0\\ \mathbf{T}^{w3} & 0\\ 0 & \mathbf{T}^u+\mathbf{E}^u\end{bmatrix}\begin{Bmatrix}\mu^p\\ \eta^p\end{Bmatrix}, \quad (10)$$

where $\{\mu\}$, $\{\varphi\}$, and $\{\eta\}$ are the vectors of bending stress resultants, shear stress resultants, and membrane stress resultants, respectively. Superscripts $w\alpha$ and $w3$ denote the bending and shear modes, respectively.

2.5. Elastoplastic Constitutive Equations. A yield function for the elastoplastic analysis is considered here. In terms of the hardening parameter k and the stresses σ_{xy}, such yield function is stated, while in the loading process there is yielding and the stresses σ_{xy} must remain at the yield surface. We satisfy the following equation:

$$\Phi\left(\sigma_{xy}\right) = f\left(\sigma_{xy}\right) - \Psi(k) = \sigma_e - \sigma_0, \tag{11}$$

where σ_0 is the uniaxial yield stress and σ_e is the equivalent stress using von Mises yield criteria. In our case, for an elastic-perfectly plastic material, $k = 0$. Recalling that we are applying the Reissner theory for the case when the membrane and moment stresses exist at the same time, the aforementioned values can be written as [38]

$$\sigma_e = \frac{1}{h}\eta_e + \frac{4}{h^2}\mu_e, \tag{12}$$

$$\sigma_0 = \frac{1}{h}\eta_0 + \frac{4}{h^2}\mu_0. \tag{13}$$

In the abovementioned equations (12) and (13), the equivalent membrane and moment stress are represented by η_e and μ_e, respectively. The uniaxial membrane and moment stress are designated by the letter η_0 and μ_0, respectively. Equations (12) and (13) are shown in [18]. When the equivalent stress σ_e reaches the yield stress, there is yielding in the whole cross section at the same time. After yielding, the behavior of the stress-strain relationship is characterized incrementally as

$$\mathrm{d}\mu_{xy} = C^{ep}_{xy\gamma\theta}\mathrm{d}\chi_{\gamma\theta} - \frac{1}{\gamma'} C_{xy\mu\rho}a_{\mu\rho}a_{\eta\zeta}\delta_{\eta\zeta}, \tag{14}$$

$$\mathrm{d}\eta_{xy} = C^{ep}_{xy\gamma\theta}\mathrm{d}\varepsilon_{\gamma\theta} - \frac{1}{\gamma'} C_{xy\mu\rho}a_{\mu\rho}a_{\eta\zeta}\delta_{\eta\zeta}, \tag{15}$$

where

$$C^{ep}_{xy\gamma\theta} = C_{xy\gamma\theta} - \frac{1}{\gamma'} C_{xy\mu\rho}a_{\mu\rho}a_{\eta\zeta}C_{\eta\zeta\gamma\theta}, \tag{16}$$

where, $C_{xy\gamma\theta}$ represents the components of fourth order isotropic tensor of elastic constants, γ' and $a_{\gamma\theta}$, which are given by

$$\begin{aligned} \gamma' &= a_{xy}C_{xy\gamma\theta}a_{\gamma\theta} + \mathbf{H}', \\ a_{\gamma\theta} &= \frac{\partial\Phi}{\partial\mu_{\gamma\theta}}, \end{aligned} \tag{17}$$

for moment and for membrane, and $a_{\gamma\theta}$ can be stated as

$$a_{\gamma\theta} = \frac{\partial\Phi}{\partial\eta_{\gamma\theta}}, \tag{18}$$

where $\mathbf{H}' = \partial\Psi/\partial\chi^p_e$ for moment and $\mathbf{H}' = \partial\Psi/\partial\varepsilon^p_e$ for membrane. $\mathbf{H}'$ is called the slope of the stress-plastic strain curve.

The additional equations required to calculate the nonlinear term due to large deflection are given by

$$\begin{aligned} w_{3,\gamma}(\mathbf{X}') + \int_\Gamma P^*_{3j,\gamma}(\mathbf{X}',\mathbf{x})w_j(\mathbf{x})\mathrm{d}\Gamma &= \int_\Gamma W^*_{3j,\gamma}(\mathbf{X}',\mathbf{x})p_j(\mathbf{x})\mathrm{d}\Gamma \\ &\quad - \int_\Omega W^*_{33,\gamma x}(\mathbf{X}',\mathbf{X})\left(\eta_{xy}w_{3,y}\right) \\ &\quad \times(\mathbf{X})\mathrm{d}\Omega \\ &\quad + \int_\Omega W^*_{33,\gamma}(\mathbf{X}',\mathbf{X})q_3(\mathbf{X})\mathrm{d}\Omega, \\ \eta^{nl}_{xy} &= B\frac{1-\nu}{2}\Big(w_{3,y}w_{3,x} \\ &\quad + \frac{\nu}{1-\nu}w_{3,y}w_{3,y}\delta_{xy}\Big). \end{aligned} \tag{19}$$

2.6. Solution Algorithm. By applying the total increment method, as Wen et al. [13] proposed, it is possible to linearize the nonlinear integral equations. An incremental procedure for the method is divided in several steps as follows: firstly, the terms considering plasticity and large deflections are zero, and then in the $(k-1)$th step, the approximations of the nonlinear terms are calculated for the kth step using the following equations:

$$\begin{aligned} \left(\eta_{\gamma y}w_{3,y}\right)_k &= \left(\eta_{\gamma y}w_{3,y}\right)_{k-1}, \\ \left(\eta^{nl}_{\gamma y}\right)_k &= \left(\eta^{nl}_{\gamma y}\right)_{k-1}, \\ \left(\mu^p\right)_k &= \left(\mu^p\right)_{k-1}, \\ \left(\eta^p\right)_k &= \left(\eta^p\right)_{k-1}. \end{aligned} \tag{20}$$

To evaluate the plastic zone of the model, the von Misses criterion is used.

By considering that,

$$\begin{aligned} \mu^e_{xy} &= \mu_{xy} + \mu^p_{xy}, \\ \eta^e_{xy} &= \eta_{xy} + \eta^p_{xy}. \end{aligned} \tag{21}$$

Equation (10) can be written as

$$\begin{aligned} \begin{Bmatrix} \mu \\ \varphi \\ \eta \end{Bmatrix} &= -\begin{bmatrix} \mathbf{H}^{wx} & 0 \\ \mathbf{H}^{w3} & 0 \\ 0 & \mathbf{H}^u \end{bmatrix}\begin{Bmatrix} w \\ u \end{Bmatrix} + \begin{bmatrix} \mathbf{G}^{wx} & 0 \\ \mathbf{G}^{w3} & 0 \\ 0 & \mathbf{G}^u \end{bmatrix}\begin{Bmatrix} p \\ t \end{Bmatrix} + \begin{Bmatrix} b^x \\ b^3 \\ 0 \end{Bmatrix} \\ &\quad - \begin{bmatrix} \mathbf{B}^{wx} & 0 \\ \mathbf{B}^{w3} & 0 \\ 0 & \mathbf{B}^u \end{bmatrix}\begin{Bmatrix} \eta_{\gamma y}w_{3,y} \\ \eta^{nl}_{\gamma y} \end{Bmatrix} \\ &\quad + \begin{bmatrix} \mathbf{T}^{wx} + \mathbf{E}^{wx} + \mathbf{I} & 0 \\ \mathbf{T}^{w3} & 0 \\ 0 & \mathbf{T}^u + \mathbf{E}^u + \mathbf{I} \end{bmatrix}\begin{Bmatrix} \mu^p \\ \eta^p \end{Bmatrix}, \end{aligned} \tag{22}$$

where μ^e and η^e are elastic moment stress resultant and elastic membrane stress resultant, respectively and $\mathbf{I}$ is an identity matrix.

After calculating all the matrices and known vectors for every load step, the following system matrices are solved.

$$[A]\{\chi\} = \{\mathbf{f}\} - \begin{bmatrix} \mathbf{B}^w & 0 \\ 0 & \mathbf{B}^u \end{bmatrix} \begin{Bmatrix} \eta_{\gamma y} w_{3,y} \\ \eta^{nl}_{\gamma y} \end{Bmatrix} + \begin{bmatrix} \mathbf{T}^w & 0 \\ 0 & \mathbf{T}^u \end{bmatrix} \begin{Bmatrix} \mu^p + \Delta\mu^p \\ \eta^p + \Delta\eta^p \end{Bmatrix},$$

$$\begin{Bmatrix} \mu^e \\ \varphi^e \\ \eta^e \end{Bmatrix} = -\begin{bmatrix} \mathbf{H}^{wx} & 0 \\ \mathbf{H}^{w3} & 0 \\ 0 & \mathbf{H}^u \end{bmatrix} \begin{Bmatrix} w \\ u \end{Bmatrix} + \begin{bmatrix} \mathbf{G}^{wx} & 0 \\ \mathbf{G}^{w3} & 0 \\ 0 & \mathbf{G}^u \end{bmatrix} \begin{Bmatrix} p \\ t \end{Bmatrix} + \begin{Bmatrix} b^x \\ b^3 \\ 0 \end{Bmatrix} - \begin{bmatrix} \mathbf{B}^{wx} & 0 \\ \mathbf{B}^{w3} & 0 \\ 0 & \mathbf{B}^u \end{bmatrix} \begin{Bmatrix} \eta_{\gamma y} w_{3,y} \\ \eta^{nl}_{\gamma y} \end{Bmatrix} + \begin{bmatrix} \mathbf{T}^{wx} + \mathbf{E}^{wx} + \mathbf{I} & 0 \\ \mathbf{T}^{w3} & 0 \\ 0 & \mathbf{T}^u + \mathbf{E}^u + \mathbf{I} \end{bmatrix} \begin{Bmatrix} \mu^p + \Delta\mu^p \\ \eta^p + \Delta\eta^p \end{Bmatrix}, \quad (23)$$

where $\Delta\mu^p$ and $\Delta\eta^p$ denote the increment plastic resultants.

The nonlinear terms due to plasticity can be calculated as shown by Karam and Telles [16]. Assuming an incremental fictitious "elastic moment and membrane" we have

$$d\mu^e_{xy} = C_{xy\gamma\theta} d\chi_{\gamma\theta}, \quad (24)$$

$$d\eta^e_{xy} = C_{xy\gamma\theta} d\varepsilon_{\gamma\theta}. \quad (25)$$

Taking into account equations (14), (15), (24), and (25), the folloeing equationscan be written as

$$d\mu_{xy} = d\mu^e_{xy} - \frac{1}{\gamma'} C_{xy\mu\rho} a_{\mu\rho} a_{\varsigma\zeta} d\mu^e_{\varsigma\zeta},$$
$$d\eta_{xy} = d\eta^e_{xy} - \frac{1}{\gamma'} C_{xy\mu\rho} a_{\mu\rho} a_{\varsigma\zeta} d\eta^e_{\varsigma\zeta}. \quad (26)$$

A procedure to compute the nonlinear terms due to plasticity is showed in the following flowchart (see Figure 1).

3. Verification

To verify the results obtained with BEM, we compared the results against FEM, specifically with the ABAQUS software. So, we analyzed a square plate with dimensions of 1.0 m per side, thickness of 0.05 m an elastic modulus of 200,000 MPa, and a Poisson's ratio of 0.3. The plate was simulated simply supported on all its sides with a uniform load of 100 ton-force applied on the complete surface of the squared plate of 1.0 m (see Figure 2). In this plate, we did the analysis for the combination of plasticity and large deformation. Both analyzes according to the graphs are in good agreement as shown in Figure 2. The results correspond to the node in the middle of the plate which is the most critical.

After comparing these two results, we conclude our code is reliable and good enough to do any kind of analysis for such combination.

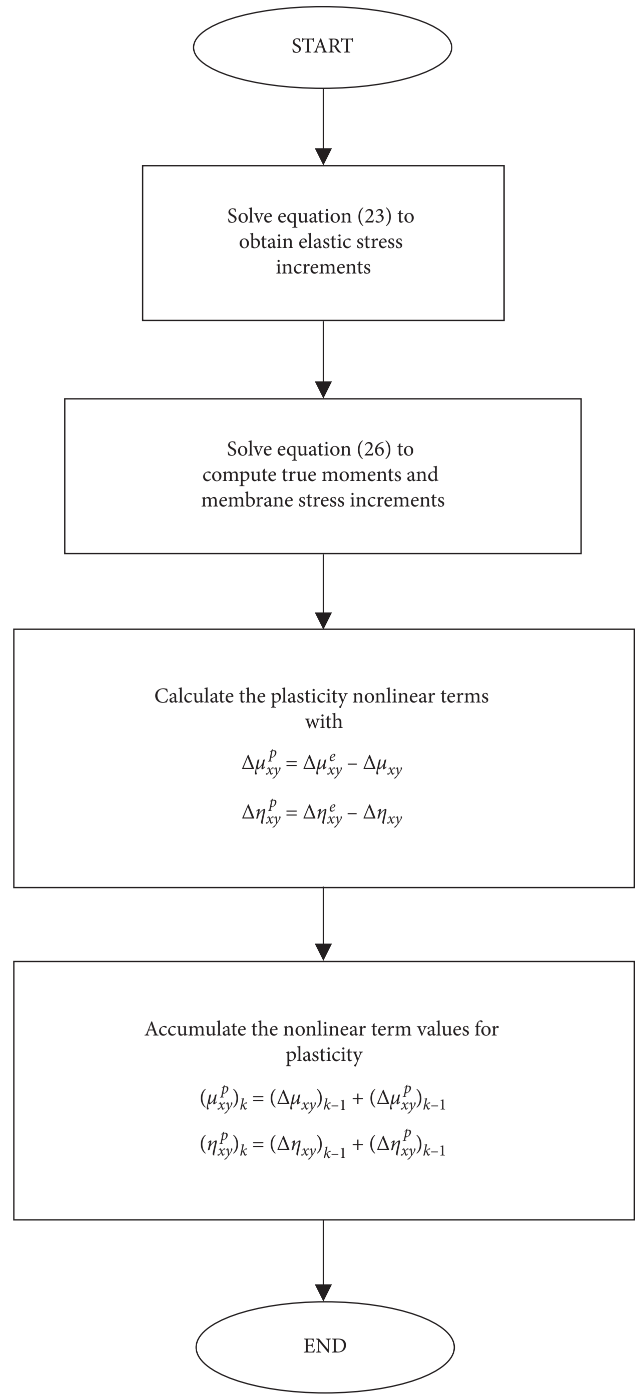

Figure 1: Procedure to calculate the nonlinear terms due to plasticity.

4. Fragility Curves

The structural elements are made to resist a certain design load which is commonly an extraordinary load established by the technical regulation of the site. The response of the structural element due to this load can be expressed in terms of displacements, shear, fatigue, stresses, and so on, which commonly are known as damage indicators. In the case of structural elements subjected to loads that could be variable in duration, magnitude, occurrence, direction, and so on, it

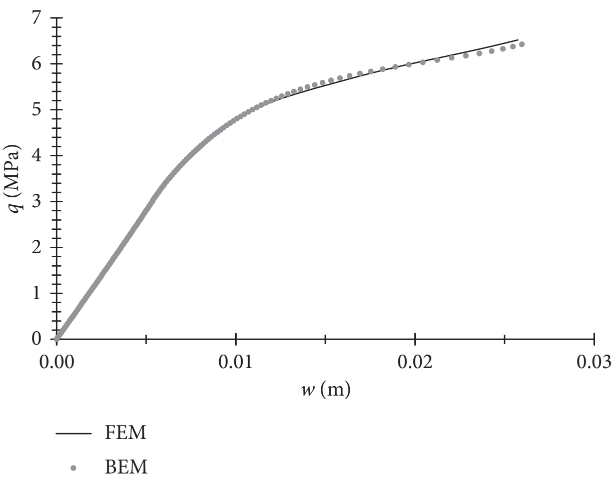

Figure 2: Verification between FEM and BEM for a square plate.

is important to know the probability of exceeding certain damage state. This allows the redesign of the structural element in order to maintain the structural element in acceptable performance levels.

A fragility curve can be defined as a graphical representation that relates the probability of exceeding a certain damage state for a given load. Both parameters, load, q, and damage state, d, are defined in accordance to the specific problem. Then, the structural response for a given load is defined in this study as the structural demand, D. Considering that the structural demand, D, follows a lognormal distribution [39], the representation of the fragility curve is as follows:

$$P[D \geq d \mid q] = 1 - \Phi\left(\frac{\ln(d) - \ln(\overline{D})}{\sigma_{\ln \overline{D}}}\right), \tag{27}$$

where Φ is the standard normal cumulative distribution function; $\overline{D}$ is the mean value of the natural logarithm of the structural demand; and $\sigma_{\ln(\overline{D})}$ is the standard deviation of the natural logarithm of the structural demand.

5. Illustrative Example

Fragility curves of a plate are estimated considering the uncertainties in its geometrical properties (thickness, length, and width) and mechanical properties (yielding, ultimate stress, and modulus of elasticity). The nominal geometric properties are the dimensions of the plate are 1.0 m wide, a, by 1.0 m long, b, with a thickness, h, equal to 0.05 m (see Figure 3). In case of the nominal mechanic properties such as the yield stress, σ_Y, is 250 MPa, the ultimate stress, σ_U, is 400 MPa, the Poisson coefficient, ν, is 0.3, and the modulus of elasticity, E, equal to 200,000 MPa. Based on the mentioned nominal properties and the statistical parameters reported by [40, 41] (see Table 1), it is possible to simulate different cases by taking into account the mean and the coefficient of variation for each parameter that is associated to a different type of distribution. The Monte Carlo method was used to simulate the study cases [42]. Moreover, it is noticed in Table 1 that the mean of each parameter is

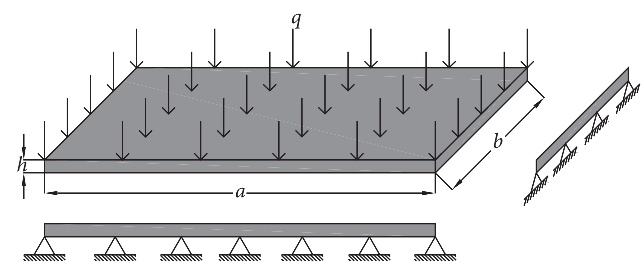

Figure 3: Schematic representation of the plate with the loading and boundary conditions.

Table 1: Statistical parameters used in the present study.

Nominal	Mean	Coefficient of variation	Type of distribution
h	1.05 h	0.044	Lognormal
a	0.988 a	0.046	Lognormal
E	0.987 E	0.076	Lognormal
Fy	1.3 Fy	0.124	Normal
Fu	1.05 Fu	0.075	Normal

estimated by means of multiplying the nominal parameter by a certain constant. These constants were reported in [40, 41].

Figure 4 shows the results obtained by the present formulation. As previously mentioned, by using the Monte Carlo method considering both the nominal properties and the statistical parameters in Table 1, a number of 100 different plates were simulated. The variability of each plate corresponds with the specific uncertainty expressed in terms of the coefficient of variation that reports each parameter in Table 1. According to this , Figure 4 shows that the 100 simulated cases presented differences in their behavior due to the fact of considering the uncertainties in mechanical and geometrical properties in which w is the deflection at the center point of the plate and q is the uniform load. This figure shows the deflection calculated at the center of the plate for 100 simulated cases. Also, it is noticed that the applied load that represents the yield of displacement of the cases varies between 3.9-7.6 MPa while the inelastic behavior due to the effect of the combined large deformations and plasticity are presented between 0.03-0.07 m.

Figure 5 shows the fragility curves obtained by using equation (27), it is noticed that the x-axis is represented in terms of the incremental uniform load, q, that the plate is subjected. Moreover, different damage states in terms of displacement, d, are selected in order to estimate the probability the structural demand, D, is greater than a certain damage state, d, for a given load measure, q. Figure 5 shows that there is a high probability of exceeding the different damage states, w, as the load, q, increases. Also, Figure 5 shows that the probability equal to 1 is reached for the damage state equal to 0.005. This implies that there is a certain probability of exceeding the mentioned damage states with a value equal to 1 (safe event). The rest of the selected damage states (i.e., 0.01 to 0.07) present a null probability that the safe event, $P[D \geq d \mid q]$, can be presented.

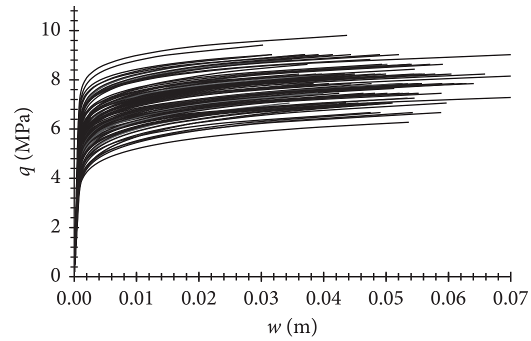

Figure 4: Deflection in the center of the plate with uniform load.

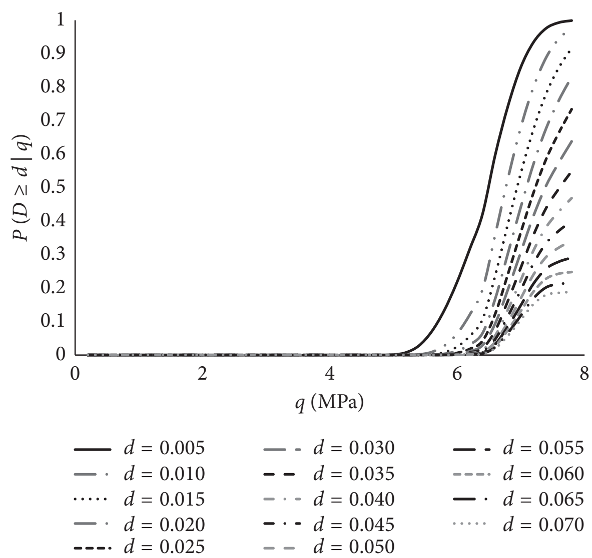

Figure 5: Fragility curves for different thresholds.

6. Conclusions

Fragility curves were estimated using the Boundary Element Method that considers the nonlinear problem of plasticity and large deformations. The classical theory of plasticity and a formulation of initial stresses that allow the formulation of integral boundary equations due to plasticity, were used. For the calculation of the plastic zone, the von Mises criterion was also used.

The obtained fragility curves consider the uncertainties in both geometrical and mechanical characteristics in order to estimate the probability that the structural demand exceeded different damage states, for a given load. The results indicate that there is a probability that certain selected damage states could be exceeding. Moreover, the approach provides information to the structural engineers about the load that produces a certain probability of exceeding each damage states.

Indicial notation is used throughout this work. Indices x and y vary from 1 to 2; indices i, j, and k vary from 1 to 3; index θ vary from 1 to 2. The following symbology is used throughout the paper:

Abbreviations

μ_{xy}: Moment stress resultant
μ_{xy}^{p}: Moment stress resultant nonlinear term
η_{xy}: Membrane stress resultant
$\mu_{xy,x}$: Moment stress resultant derivative
$\eta_{xy,y}$: Membrane stress resultant derivative
B: Tension stiffness
C: Shear stiffness
D: Bending stiffness
η_{xy}^{p}: Membrane stress resultant nonlinear term
φ_x: Shear stress resultant
$\varphi_{x,x}$: Shear stress resultant derivative
χ_{xy}: Generalized displacements in direction 1
δ_{xy}: Kronecker delta function
ε_{xy}: Generalized displacements in direction 2
γ_{x3}: Generalized displacements in direction 3
ν: Poisson's rate
q_3: Uniform load
c_{ij}: Jump term
w_x: Two rotations in plate
w_3: Deflection in plate
u_x: Displacements in-plane
Γ: Boundary of the plate
p_j: Generalized tractions
Ω: Domain of the plate
$U_{\theta x}^{*}$: Weighting functions
$\mathbf{H}$: Boundary element influence matrix
$\mathbf{G}$: Boundary element influence matrix
$\mathbf{B}$: Influence matrices for large deflection
$\mathbf{T}$: Influence matrices for plasticity
b: Load rate vectors
$[A]$: System matrix
$\{\mathbf{f}\}$: Vector of prescribed boundary values
Φ: Shape functions
W_{i3}: Plate bending displacement fundamental solutions for displacement integral equations
σ_{xy}: Normal and shear stresses
$\Psi(k)$: Yield stress as a function of a hardening parameter k
h: Thickness of the plate
$C_{xy\gamma\theta}$: Components of fourth order isotropic tensor of elastic constants
$\mathbf{I}$: Identity matrix
$W_{ij}^{*}(\mathbf{X}', \mathbf{x})$: Fundamental solution of displacement
$P_{ij}^{*}(\mathbf{X}', \mathbf{x})$: Fundamental solution of traction
$\chi_{ixy}^{*}(\mathbf{X}', \mathbf{X})$: Fundamental solution of strains
$U_{\theta x}^{*}(\mathbf{X}', \mathbf{x})$: Fundamental solution of displacement on membrane
$T_{\theta x}^{*}(\mathbf{X}', \mathbf{x})$: Fundamental solution of traction on membrane
$\varepsilon_{\theta xy}^{*}(\mathbf{X}', \mathbf{X})$: Fundamental solution of strains on membrane
P: Probability of failure
D: Structural demand
d: Damage state
p: Load measure

Φ: Standard normal cumulative distribution function
$\overline{D}$: Mean value of the natural logarithm of the structural demand.

Data Availability

The data used to support the findings of this study are available from the corresponding author upon request.

Conflicts of Interest

The authors declare no conflicts of interest regarding the publication of this paper.

Acknowledgments

This research has been supported by CONACYT through the support given under project number 240413. The first and fourth authors thank the Instituto Politécnico Nacional for the economic support; the second author thanks CONACYT for the economic support during his PhD studies; and the third author thanks Universidad Autónoma Metropolitana for the economic support.

References

[1] G. Kirchhoff, "Über das gleichgewicht und die bewegung einer elastischen scheibe," *Journal für die Reine und Angewandte Mathematik*, vol. 1850, no. 40, pp. 51–88, 1850.
[2] M. Ben-Amoz, "On a variational theorem in coupled thermoelasticity," *Journal of Applied Mechanics*, vol. 32, no. 4, pp. 943–945, 1965.
[3] M. H. Aliabadi, "The boundary element method. Volume 2: applications in solids and structures," *Bautechnik*, vol. 80, no. 2, pp. 138-139, 2003.
[4] M. Stern, "A general boundary integral formulation for the numerical solution of plate bending problems," *International Journal of Solids and Structures*, vol. 15, no. 10, pp. 769–782, 1979.
[5] F. Hartmann and R. Zotemantel, "The direct boundary element method in plate bending," *International Journal for Numerical Methods in Engineering*, vol. 23, no. 11, pp. 2049–2069, 1986.
[6] F. V. Weeën, "Application of the boundary integral equation method to Reissner's plate model," *International Journal for Numerical Methods in Engineering*, vol. 18, no. 1, pp. 1–10, 1982.
[7] V. J. Karam and J. C. F. Telles, "On boundary elements for Reissner's plate theory," *Engineering Analysis with Boundary Elements*, vol. 5, no. 1, pp. 21–27, 1988.
[8] M. H. Aliabadi, "Plate bending analysis with boundary element," *Computational Mechanics*, vol. 2, 1998.
[9] T. Q. Ye and Y. Liu, "Finite deflection analysis of elastic plate by the boundary element method," *Applied Mathematical Modelling*, vol. 9, no. 3, pp. 183–188, 1985.
[10] M. Tanaka, "Large deflection analysis of thin elastic plates," *Developments in Boundary Element Methods*, vol. 3, pp. 115–136, Elsevier Applied Science Publishers, London, UK, 1984.
[11] N. Kamiya and Y. Sawaki, "An integral equation approach to finite deflection of elastic plates," *International Journal of Non-Linear Mechanics*, vol. 17, no. 3, pp. 187–194, 1982.
[12] X.-Y. Lei, M.-K. Huang, and X. Wang, "Geometrically nonlinear analysis of a Reissner type plate by the boundary element method," *Computers & Structures*, vol. 37, no. 6, pp. 911–916, 1990.
[13] P. H. Wen, M. H. Aliabadi, and A. Young, "Large deflection analysis of Reissner plate by boundary element method," *Computers & Structures*, vol. 83, no. 10-11, pp. 870–879, 2005.
[14] J. Purbolaksono and M. H. Aliabadi, "Large deformation of shear-deformable plates by the boundary-element method," *Journal of Engineering Mathematics*, vol. 51, no. 3, pp. 211–230, 2005.
[15] T. Dirgantara and M. H. Aliabadi, "A boundary element formulation for geometrically nonlinear analysis of shear deformable shells," *Computer Methods in Applied Mechanics and Engineering*, vol. 195, no. 33–36, pp. 4635–4654, 2006.
[16] V. J. Karam and J. C. F. Telles, "Nonlinear material analysis of Reissner's plates," in *Plate Bending Analysis with Boundary Element*, pp. 127–163, Computational Mechanics Publications, Southampton, UK, 1998.
[17] A. Chandra and S. Mukherjee, "Applications of the boundary element method to large strain large deformation problems of viscoplasticity," *The Journal of Strain Analysis for Engineering Design*, vol. 18, no. 4, pp. 261–270, 1983.
[18] Supriyono and M. H. Aliabadi, "Analysis of shear deformable plates with combined geometric and material nonlinearities by boundary element method," *International Journal of Solids and Structures*, vol. 44, no. 3-4, pp. 1038–1059, 2007.
[19] S. Rahman and G. Chen, "Continuum shape sensitivity and reliability analyses of nonlinear cracked structures," *International Journal of Fracture*, vol. 131, no. 2, pp. 189–209, 2005.
[20] X. Huang and M. H. Aliabadi, "Probabilistic fracture mechanics by the boundary element method," *International Journal of Fracture*, vol. 171, no. 1, pp. 51–64, 2011.
[21] C. Su and C. Zheng, "Probabilistic fracture mechanics analysis of linear-elastic cracked structures by spline fictitious boundary element method," *Engineering Analysis with Boundary Elements*, vol. 36, no. 12, pp. 1828–1837, 2012.
[22] C. Su, S. Zhao, and H. Ma, "Reliability analysis of plane elasticity problems by stochastic spline fictitious boundary element method," *Engineering Analysis with Boundary Elements*, vol. 36, no. 2, pp. 118–124, 2012.
[23] C. Su and J. Xu, "Reliability analysis of Reissner plate bending problems by stochastic spline fictitious boundary element method," *Engineering Analysis with Boundary Elements*, vol. 51, pp. 37–43, 2015.
[24] M. Ettouney, H. Benaroya, and J. Wright, "Boundary element methods in probabilistic structural analysis (PBEM)," *Applied Mathematical Modelling*, vol. 13, no. 7, pp. 432–441, 1989.
[25] I. Kaljević and S. Saigal, "Stochastic boundary elements in elastostatics," *Computer Methods in Applied Mechanics and Engineering*, vol. 109, no. 3-4, pp. 259–280, 1993.
[26] M. Kaminski, "Stochastic second-order BEM perturbation formulation," *Engineering Analysis with Boundary Elements*, vol. 23, no. 2, pp. 123–129, 1999.
[27] M. Kamiński, "Application of the generalized perturbation-based stochastic boundary element method to the elastostatics," *Engineering Analysis with Boundary Elements*, vol. 31, no. 6, pp. 514–527, 2007.
[28] D. W. Kim and B. M. Kwak, "Reliability-based shape optimization of two-dimensional elastic problems using BEM," *Computers & Structures*, vol. 60, no. 5, pp. 743–750, 1996.

[29] B. S. Thompson, "On a variational theorem in acousto-elastodynamics," *Journal of Sound and Vibration*, vol. 83, no. 4, pp. 461–477, 1982.

[30] K. R. Karim and F. Yamazaki, "Effect of isolation on fragility curves of highway bridges based on simplified approach," *Soil Dynamics and Earthquake Engineering*, vol. 27, no. 5, pp. 414–426, 2007.

[31] G. C. Marano, R. Greco, and M. Mezzina, "Stochastic approach for analytical fragility curves," *KSCE Journal of Civil Engineering*, vol. 12, no. 5, pp. 305–312, 2008.

[32] C. Mai, K. Konakli, and B. Sudret, "Seismic fragility curves for structures using non-parametric representations," *Frontiers of Structural and Civil Engineering*, vol. 11, no. 2, pp. 169–186, 2017.

[33] S. Cui, C. Guo, J. Su, E. Cui, and P. Liu, "Seismic fragility and risk assessment of high-speed railway continuous-girder bridge under track constraint effect," *Bulletin of Earthquake Engineering*, vol. 17, no. 3, pp. 1639–1665, 2019.

[34] M. G. Stewart, P. C. Ryan, D. J. Henderson, and J. D. Ginger, "Fragility analysis of roof damage to industrial buildings subject to extreme wind loading in non-cyclonic regions," *Engineering Structures*, vol. 128, pp. 333–343, 2016.

[35] X. Fu, H. N. Li, L. Tian, J. Wang, and H. Cheng, "Fragility analysis of transmission line subjeted to wind loading," *Journal of Performance of Constructed Facilities*, vol. 33, no. 4, Article ID 04019044, 2019.

[36] C. Petrone, T. Rossetto, and K. Goda, "Fragility assessment of a RC structure under tsunami actions via nonlinear static and dynamic analyses," *Engineering Structures*, vol. 136, pp. 36–53, 2017.

[37] Supriyono and M. H. Aliabadi, "Boundary element method for shear deformable plates with combined geometric and material nonlinearities," *Engineering Analysis with Boundary Elements*, vol. 30, no. 1, pp. 31–42, 2006.

[38] T. Dirgantara and M. H. Aliabadi, "Elastoplastic boundary element method for shear deformable shells," *Engineering Structures*, vol. 45, pp. 62–67, 2012.

[39] E. Rosenblueth and L. Esteva, "Reliability basis for some Mexican codes," *American Concrete Institute*, vol. 31, pp. 1–42, 1972.

[40] A. E. Mansour, H. Y. Jan, C. I. Zigelman, Y. N. Chen, and S. J. Harding, "Implementation of reliability methods to marine structures," *Transactions Society of Naval Architects and Marine Engineers*, vol. 92, pp. 353–382, 1984.

[41] T. V. Galambos and M. K. Ravindra, "Properties of steel for use in LRFD," *Journal of the Structural Engineering Division*, vol. 104, no. 9, pp. 1459–1468, 1978.

[42] H. Tanizaki, *Computational Methods in Statistics and Econometrics*, Marcel Dekker Inc., New York, NY, USA, 2004.

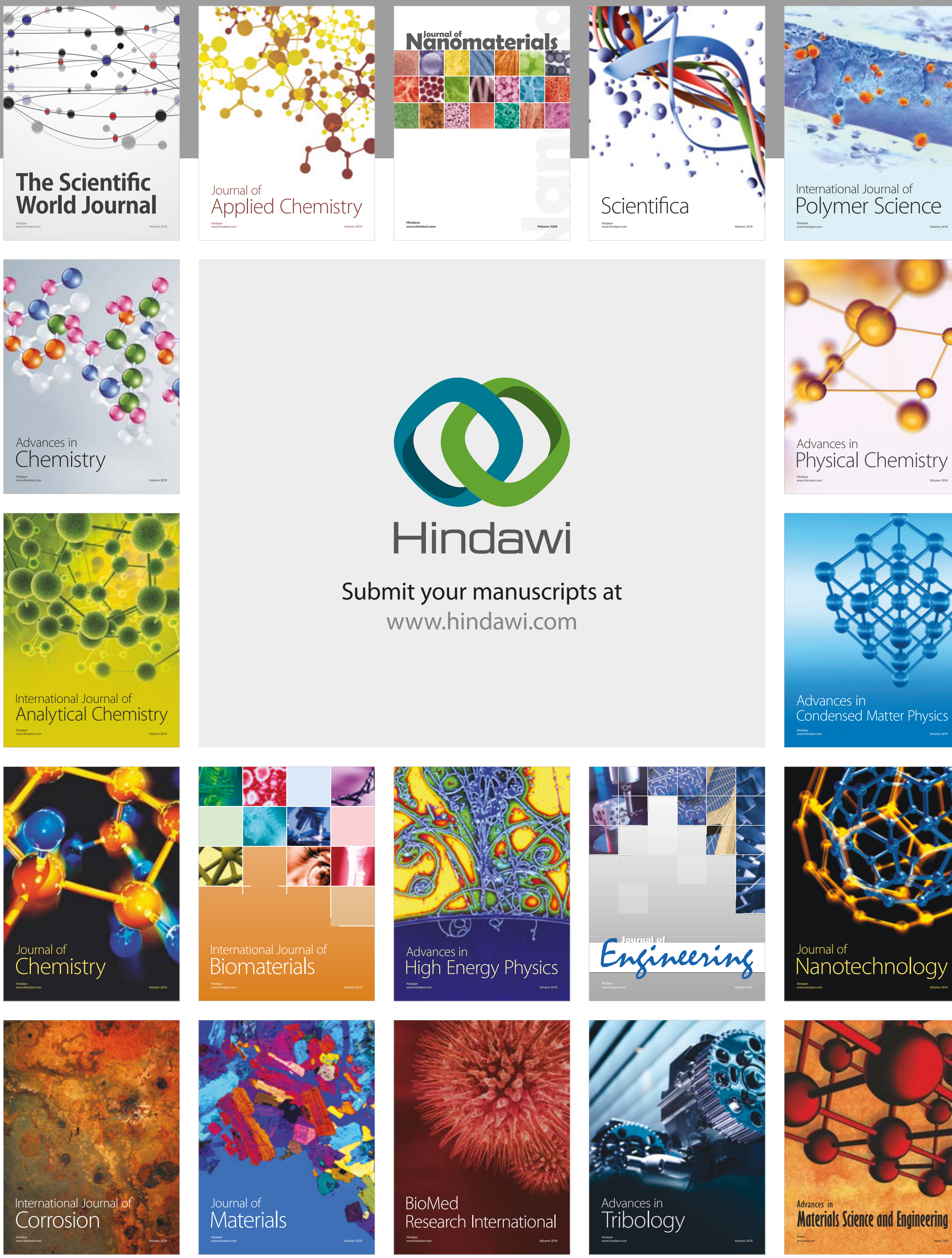
The Scientific World Journal
Journal of Applied Chemistry
Journal of Nanomaterials
Scientifica
International Journal of Polymer Science
Advances in Chemistry
Hindawi
Submit your manuscripts at
www.hindawi.com
Advances in Physical Chemistry
International Journal of Analytical Chemistry
Advances in Condensed Matter Physics
Journal of Chemistry
International Journal of Biomaterials
Advances in High Energy Physics
Journal of Engineering
Journal of Nanotechnology
International Journal of Corrosion
Journal of Materials
BioMed Research International
Advances in Tribology
Advances in Materials Science and Engineering